Resolution enhancement of Hyperion hyperspectral data using Ikonos multispectral data

Edwin M. Winter*
Technical Research Associates, Inc., Honolulu, HI 96822

Michael E. Winter
University of Hawaii, Honolulu, HI 96822

Scott G. Beaven
Space Computer Corp, Los Angeles, CA 90025

Anthony J. Ratkowski
Air Force Research Laboratory, Hanscom AFB, MA 01731-3010

ABSTRACT

We have developed a new and innovative technique for combining a high-spatial-resolution multispectral image with a lower-spatial-resolution hyperspectral image. The approach, called CRISP, compares the spectral information present in the multispectral image to the spectral content in the hyperspectral image and derives a set of equations to approximately transform the multispectral image into a synthetic hyperspectral image. This synthetic hyperspectral image is then recombined with the original low-spatial-resolution hyperspectral image to produce a sharpened product. The result is a product that has the spectral properties of the hyperspectral image at a spatial resolution approaching that of the multispectral image. To test the accuracy of the CRISP method, we applied the method to synthetic data generated from hyperspectral images acquired with an airborne sensor. These high-spatial-resolution images were used to generate both a lower-spatial-resolution hyperspectral data set and a four-band multispectral data set. With this method, it is possible to compare the output of the CRISP process to the 'truth data' (the original scene). In all of these controlled tests, the CRISP product showed both good spectral and visual fidelity, with an RMS error less than one percent when compared to the 'truth' image. We then applied the method to real world imagery collected by the Hyperion sensor on EO-1 as part of the Hurricane Katrina support effort. In addition to multiple Hyperion data sets, both Ikonos and QuickBird data were also acquired over the New Orleans area. Following registration of the data sets, multiple high-spatial-resolution CRISP-generated hyperspectral data sets were created. In this paper, we present the results of this study that shows the utility of the CRISP-sharpened products to form material classification maps at four-meter resolution from space-based hyperspectral data. These products are compared to the equivalent products generated from the source 30m resolution Hyperion data.

Keywords: sharpening, Hyperion, hyperspectral, multispectral, Ikonos, CRISP, resolution, enhancement

1. INTRODUCTION

Hyperspectral imaging systems are receiving increasing attention for a wide variety of military, intelligence, civil and commercial systems. The reason is that a hyperspectral imager provides information on scene content that is not obtainable from single-band or multispectral sensors. In this work, we examine the benefits of combining data from high-spatial-resolution, low-spectral-resolution spectral imaging sensors with data obtained from high-spectral-resolution, low-spatial-resolution spectral imaging sensors. The deployment of a high-spatial-resolution space-based

* Correspondence: email: edwinter@tracam.com

Report Documentation Page

Form Approved
OMB No. 0704-0188

1. REPORT DATE	2. REPORT TYPE	3. DATES COVERED
01 SEP 2007	**N/A**	**-**

4. TITLE AND SUBTITLE	5a. CONTRACT NUMBER
Resolution enhancement of Hyperion hyperspectral data using Ikonos multispectral data	5b. GRANT NUMBER
	5c. PROGRAM ELEMENT NUMBER
6. AUTHOR(S)	5d. PROJECT NUMBER
	5e. TASK NUMBER
	5f. WORK UNIT NUMBER
7. PERFORMING ORGANIZATION NAME(S) AND ADDRESS(ES) **Technical Research Associates, Inc., Honolulu, HI 96822**	8. PERFORMING ORGANIZATION REPORT NUMBER
9. SPONSORING/MONITORING AGENCY NAME(S) AND ADDRESS(ES)	10. SPONSOR/MONITOR'S ACRONYM(S)
	11. SPONSOR/MONITOR'S REPORT NUMBER(S)

12. DISTRIBUTION/AVAILABILITY STATEMENT
Approved for public release, distribution unlimited

13. SUPPLEMENTARY NOTES

14. ABSTRACT

15. SUBJECT TERMS

16. SECURITY CLASSIFICATION OF:			17. LIMITATION OF ABSTRACT	18. NUMBER OF PAGES	19a. NAME OF RESPONSIBLE PERSON
a. REPORT	b. ABSTRACT	c. THIS PAGE			
unclassified	**unclassified**	**unclassified**	**UU**	**11**	

hyperspectral imaging sensor presents many technological challenges, among which is the requirement for a large-aperture optical system. Currently, the United States has one hyperspectral sensor in Earth orbit, the Hyperion sensor onboard the NASA EO-1 spacecraft[1]. Hyperion covers the reflective spectral regime from 400 to 2500 nm with a spatial resolution of 30 meters. The sensor has a 12.5-cm-diameter aperture and weighs approximately 50 kg. To simplify operations and keep the package size weight and power to a minimum, Hyperion acquires data by push-brooming along its ground track at the orbital rate without any image motion compensation. While adequate for terrain classification, the thirty-meter spatial resolution of the Hyperion imager is too large for the detection of some objects of interest.

Typically, the spectral imagery data from the high-spatial-resolution, low-spectral-resolution sensor and the high-spectral resolution, low-spatial-resolution sensor are treated separately. The hyperspectral imagery is a rich source of information that lends itself to both physical processing techniques, such as the linear-mixture-model-based techniques[2,3,4], and statistically based exploitation methods, such as the Principal Components (PC) transform[5] and the Minimum Noise Fraction (MNF) transform[6].

The process described herein, called "CRISP", combines information contained in a low-spatial-resolution hyperspectral image with a high-spatial-resolution multispectral/panchromatic image in such a way that the resulting image product has the spectral characteristics of the hyperspectral image and the spatial characteristics of the multispectral/panchromatic image. The result of this sharpening procedure is an image product is that fully exploitable as a hyperspectral image. This is in contrast to an image product that has only limited utility, such as one based upon intensity sharpening[7]. Using the technique we have developed, the hyperspectral processing approach can be easily extended to pairs of images with different spectral and spatial characteristics. With a high-quality spatial co-registration program, it is possible to combine data from different spectral imaging sensors. For example, commercial multispectral sensors such as Ikonos and QuickBird are currently in orbit and are providing imagery that could be used to sharpen Hyperion hyperspectral imagery. The CRISP method differs from the Color Normalization[8] method in that CN sharpening result is explicitly limited to sharpening only the bands in the hyperspectral image that are covered by the bands of the multispectral image.

2. APPROACH

Consider a simple case of vegetation detection. With a hyperspectral imager, one can create a matched filter that separates vegetation from the background. Vegetation detection in multispectral data collected with a high-spatial-resolution space-based sensor can be accomplished with the Normalized Difference Vegetation Index (NDVI) algorithm[7] that uses a normalized difference between two bands to highlight pixels with a high likelihood of vegetation content. A simple "vegetation sharpening" procedure could use the NDVI output of the high-spatial-resolution multispectral imager to increase the spatial resolution of vegetation determined from lower-spatial-resolution hyperspectral imagery data by adding a standard vegetation spectrum with an intensity related to the NDVI score. Such an approach would have a number of problems. First, only vegetation would be sharpened, which is of limited utility. Second, all vegetation in the sharpened image would be assigned the characteristics of the spectrum of the vegetation spectrum used in the sharpening.

The CRISP sharpening approach is a significantly enhanced version of the simple "NDVI sharpening" outlined above. Instead of a vegetation spectrum being applied in direct proportion to the NDVI score, the multispectral and hyperspectral images are compared statistically to derive spectral relationships between them. These relationships are not dependent on *a priori* physical knowledge of the scene but rather on the correlation of the content in the two images. Since the same physical phenomena generate data in both the multispectral image and the hyperspectral image, a strong correlation between the content in both images should be present. This correlation can be described in terms of simple linear equations that approximately relate one image to the other. In the case where there is a high percentage of vegetation in the scene, an NDVI-like metric will be deduced automatically and applied to sharpen the image in a similar way.

This relationship is then used to build a model high-spatial-resolution hyperspectral image. Since this model-sharpened image is produced using the data in the multispectral image, it has some low rank and poor statistical properties. Because the hyperspectral image already contains the spectral information at low spatial resolution, this information is used to replace the low-spatial-resolution (low-spatial-frequency) portions of the model-sharpened image. The end product therefore retains all of the spectral information from the hyperspectral image, along with the added detail deduced through the correlation between the multispectral and hyperspectral images. Information is only added during this process. The original hyperspectral image can be recovered by appropriately sub-sampling the model-sharpened image at lower spatial resolution. The added detail is solely present at the highest spatial resolution of the sharpened image.

Further detail on the CRISP algorithm is available in the references[9].

3. RESULTS

The CRISP sharpening procedure depends on the relationship between the multispectral and hyperspectral images as described by the model. The effectiveness of the sharpening process depends on the accuracy of the model-sharpened image. Since the model-sharpened image has the same spectral resolution as the hyperspectral image, its accuracy can be examined by comparing the two images. For clarity, we have used a 1997 AVIRIS[10] Cuprite, NV reflectance scene to generate a synthetic data set consisting of a low-spatial-resolution hyperspectral image and a high-spatial-resolution multispectral image. The Cuprite region has been studied extensively[11,12] and provides a well-understood test for hyperspectral image-processing techniques. While the AVIRIS Cuprite scene is available from NASA in both radiance and reflectance, we chose to use the reflectance scene because it has been extensively used for analyses and it facilitates spectral comparisons. The low-spatial-resolution hyperspectral image was generated by applying a Gaussian Blur with a width of 15 pixels to the original AVIRIS image using the commercial ENVI[13] software package. As part of our development efforts we experimented with many different hyperspectral scenes, creating in each case a low-spatial-resolution hyperspectral image and a high-spatial-resolution multispectral image from an original high-spatial resolution scene. This provided a series of controlled experiments for testing our algorithm and the software implementation since the error was directly measurable and the source of the error was the sharpening process, not registration errors or temporal changes.

The high-spatial-resolution multispectral image was generated by spectrally re-sampling the original AVIRIS Cuprite data to approximate the six bands of LANDSAT. The product of sharpening this synthetic image pair is an image with exactly the same spatial and spectral resolution of the original AVIRIS input data, so the sharpened image can be compared directly to it.

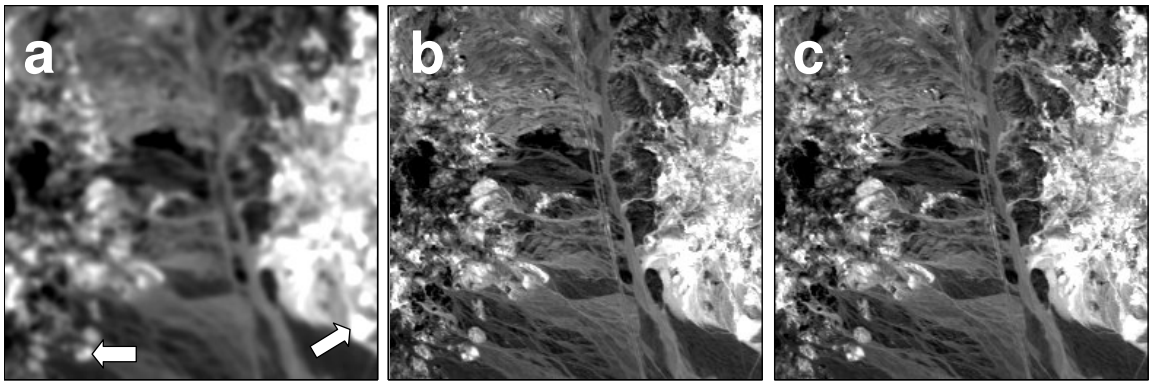

Figure 1. Three stages of the CRISP sharpening process illustrated using synthetic images generated from AVIRIS Cuprite 1997 data. A low-spatial-resolution hyperspectral image (sub-figure "a") is combined with a high-spatial-resolution multispectral image (sub-figure "b", generated by spectrally sub-sampling the HSI image). The result is shown in sub-figure "c": a hyperspectral image with the high spatial resolution of the multispectral image. The arrows indicate the regions used for spectral analysis (left arrow: Alunite, right arrow: Kaolinite).

Two spectra from the hyperspectral image were selected for examination: an Alunite spectrum and a Kaolinite spectrum. These spectra are shown in Figure 2, the black line being the original hyperspectral truth spectrum, the gray line being the model-sharpened spectrum and the dashed line being the final sharpened spectrum. In both cases, the spectra show a good match between the sharpened spectra and the original spectra. In the case of Kaolinite, the model-sharpened spectrum shows an extremely good match to the truth spectrum. There is some deviation towards the SWIR, where the model spectrum overshoots the spectral feature. This is most likely due to the fact that LANDSAT has only one band in the SWIR, which makes predicting these spectral features difficult. Nonetheless, once the low-spatial-resolution hyperspectral data are incorporated, the discrepancy disappears and there appears (subjectively) to be an excellent match. For the Alunite spectra, the agreement is less good, with both the model spectrum and the final sharpened spectrum underestimating the reflectance. This is most likely because the spatial extent of the Alunite feature is relatively small, on the order of the spatial resolution of the synthetic hyperspectral image. Note, however, that in both cases the model-sharpened spectrum contains all of the spectral features of the truth spectrum. This is a good indication that the model relating the two images is accurate.

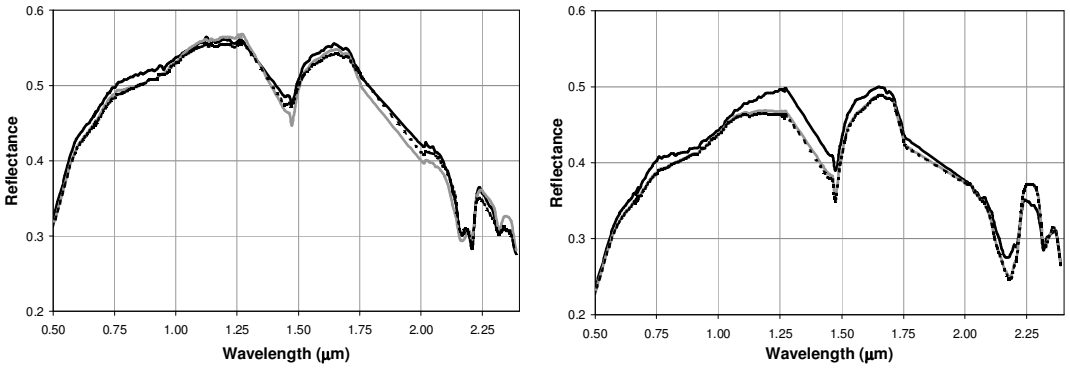

Figure 2. A comparison of three spectra from the Cuprite scene for Kaolinite (left) and Alunite (right). The three spectra for each graph represent "truth" hyperspectral (solid black) modeled spectra (gray solid) and final sharpened (dashed black). The model-sharpened data shows a very good match to the truth spectrum despite the fact that it is generated from the multispectral data

Since synthetic data was used, a comparison between the sharpened image and the parent hyperspectral image can be performed. The RMS(error) metric provides a simple means of quantifying the difference between two images. The RMS(error) is calculated by subtracting the sharpened image product from the original hyperspectral image and calculating the mean square of the result. This metric provides a single objective number quantifying the difference between the two images in data units. Figure 3 shows the mean error spectrum, with the mean image spectrum shown for comparison. The error is generally lower than one percent reflectance, with the error peaking at approximately 1.4 microns. This error peak is likely due to inaccuracies introduced in the atmospheric compensation step. At wavelengths where the atmospheric transmission is low, atmospheric compensation results in the data being multiplied by a relatively large number, increasing the noise level. Because of this, atmospheric absorption regions of a spectrum tend to have more noise than at other wavelengths.

The image fidelity of the sharpened image is also good. Figure 4 shows a small portion of the input low-spatial-resolution data, the sharpened output and the original AVIRIS data for comparison. Subjectively the sharpened data looks very similar to the original HSI data, despite being derived from the low-spatial-resolution synthetic AVIRIS image.

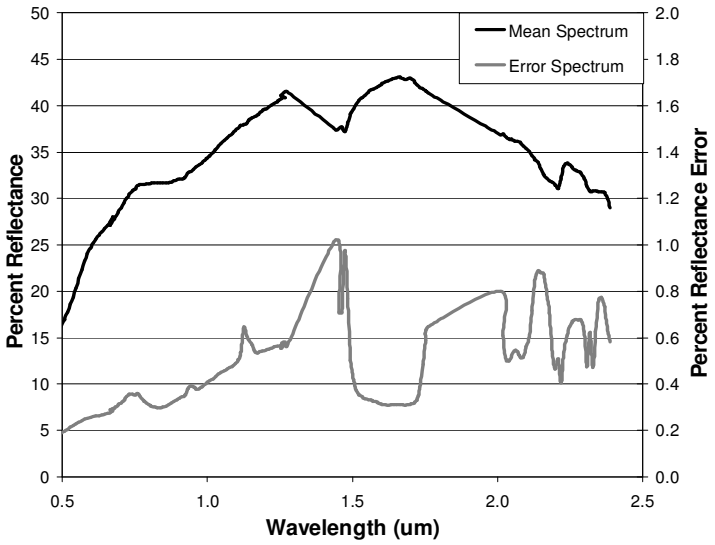

Figure 3. Error spectrum for the sharpened image. Note that the RMS error is less than one recent except for several water-dominated bands. The mean image spectrum for the AVIRIS Cuprite data set is shown for reference.

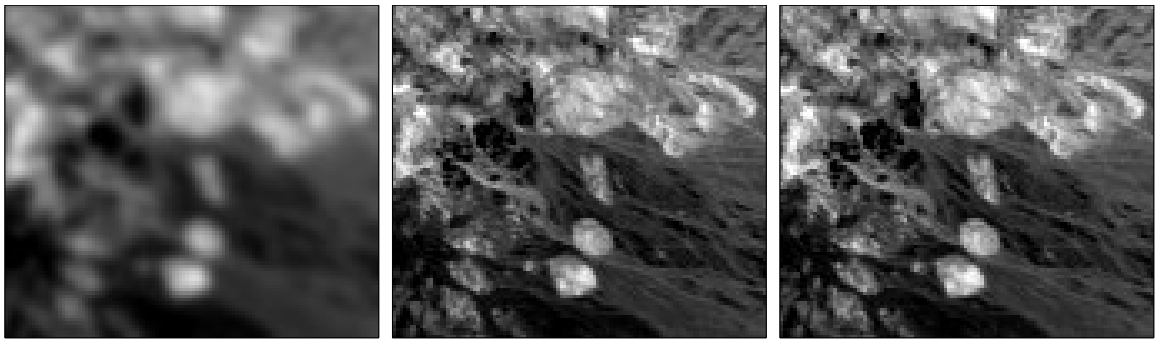

Figure 4. Detailed view of data from the sharpening experiment at 1.0 μm. Left: low-spatial-resolution HSI image generated from a 15-pixel Gaussian blur of AVIRIS Cuprite data; Middle: sharpened output; Right: the original AVIRIS scene for comparison.

4. APPLICATION TO HYPERION DATA

To demonstrate performance on real data, it is necessary to have a registered coincident and contemporary pair of hyperspectral and multispectral images. Since there was no multispectral and hyperspectral data taken from the same platform, the hyperspectral image was registered to the multispectral image using the SMART algorithm.

We chose data sets taken in support of the Hurricane Katrina relief effort because many data sets were available from many different remote-sensing satellites. All of the data sets used for this study are courtesy of the U.S. Geological Survey. We worked with four different Hyperion data sets, two Ikonos images and one QuickBird image in our sharpening studies. Since the only high-spatial-resolution multispectral data available was from the visible/near infrared

portion of the spectrum, we restricted our enhancement studies to that portion of the Hyperion data. In the following paragraphs, the registration and resolution enhancement of one Hyperion/Ikonos data pair will be discussed. This data pair consisted of Hyperion and Ikonos data taken only 51 minutes apart on 8 September 2005. This case is nearly ideal with little illumination or material changes between the multispectral and hyperspectral images. True-color images formed from the two data sets are shown in Figure 5.

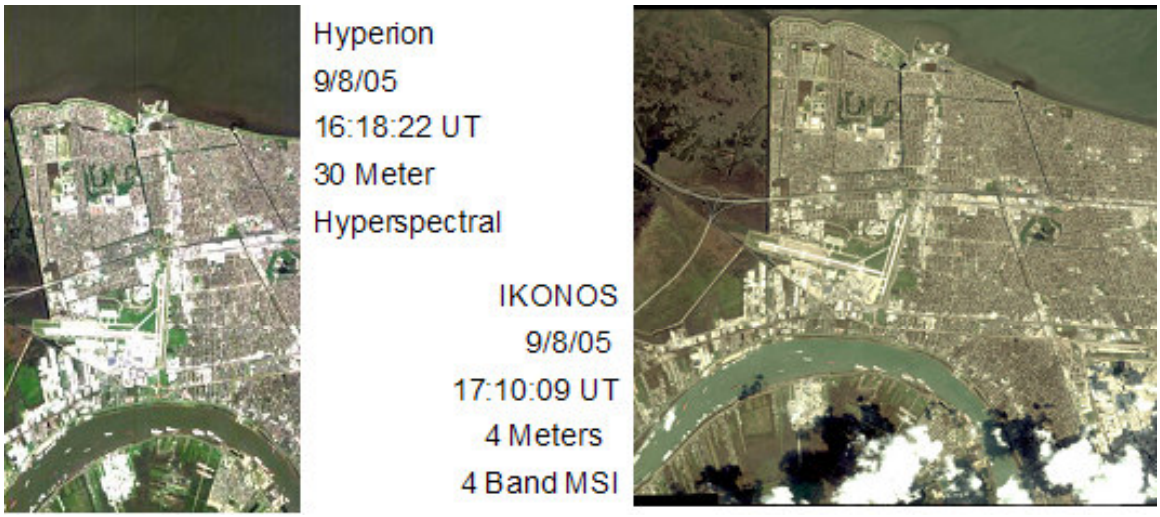

Figure 5. Hyperion and Ikonos data taken on the same day 51 minutes apart. Ikonos and Hyperion data are courtesy of the U.S. Geological Survey.

The SCC Multi-sensor Aided Registration Tool (SMART) algorithm was designed by Space Computer Corporation to register data at two different spatial scales using both available geo-coordinate data and scene-based techniques to achieve the registration accuracy necessary for the Color-Sharpening application. Generally, the two major steps in obtaining registered data pairs are as follows:

(1) Geo-registration of both sensor data sets onto geo-coordinates, typically a northing-easting grid

(2) Scene-based registration with the higher-resolution product being the reference and the coarser-resolution data up-sampled and warped to the reference.

These may be used either independently or sequentially as required to produce registered data pairs for Color Sharpening. The SMART package is focused on data sets that are of most interest for application of the Color-Sharpening process, such as handling widely varying spatial resolutions. Using Ikonos as the reference, we geo-registered the Hyperion imagery onto the same geo-grid, accounted for biases using a single tie-point and produced a re-sampled Hyperion imagery over the overlap region. This resampled Hyperion data was then used in the scene-based registration refinement step along with the Ikonos to obtain a pixel-level registered image pair that is suitable for CRISP algorithm application. Since the scene was of an urban area, of the high spatial content in both images enabled the generation of automated tie points using the scene-based algorithm's local-area phase correlation method. This same process was applied to several other Hyperion data samples that overlapped this region in the days following Hurricane Katrina. Several of these involved the registration of data taken several days apart. The area of the SMART-registered image chosen for study was an area south of Louis Armstrong Airport and included the Mississippi River. Images formed from the two data sets after SMART registration are shown in Figure 6.

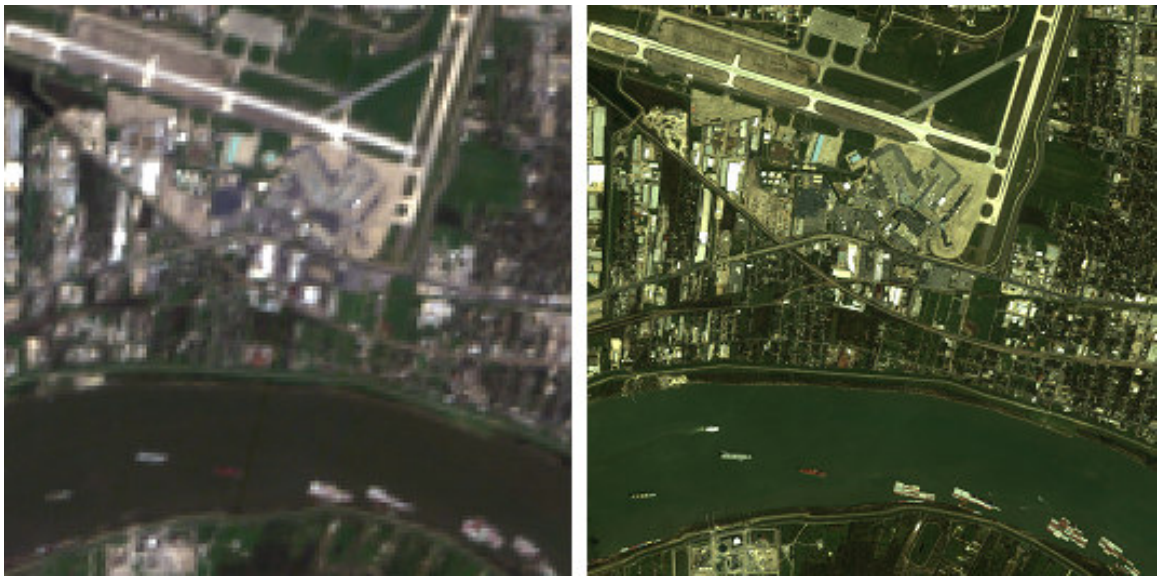

Figure 6. New Orleans Ikonos and Hyperion images after registration using the SMART software package.

Since this experiment involved real hyperspectral and multispectral data, there was no high-spatial-resolution truth data and no quantitative method, such as calculating the RMS error, to assess the accuracy of the performance of the CRISP algorithm. The procedure of forming classification maps using the N-FINDR[14] algorithm was chosen to display the results of the Color Sharpening Process. N-FINDR was used to unmix both the low-spatial-resolution Hyperion data and the Hyperion data after Color Sharpening with the high-spatial-resolution Ikonos data. N-FINDR is an autonomous endmember determination and linear unmixing program that finds the endmembers in a hyperspectral data set. Endmembers can be identified as the spectra most separated from each other in the hyperspectral data set. In the ideal case these endmembers will be pure materials, such as grass, soil, various minerals, et cetera. If there is no pure pixel of a particular material, then the endmember will be the pixel in the scene that is closest to a pure material. The N-FINDR autonomous endmember determination and unmixing algorithm can be used for terrain classification. In this case a map can be made showing the fraction of each endmember material in each pixel. The results of this process are shown in Figure 7 for one of the material-related endmembers. The material corresponds to a roofing material used on three buildings near each other. The fraction plane formed from the 30m-resolution Hyperion data is shown along with the fraction plane shown for the effectively four-meter-resolution CRISP-sharpened Hyperion data. A recent satellite image from Google[15] is shown for reference. By inspecting the N-FINDR fraction plane maps, it is apparent that the man-made structures are better resolved in the Color Sharpened fraction planes of Figure 7 than at the original resolution of Hyperion. Better edge detail and almost no bleeding of the buildings into the background can be seen in these and other fraction planes. This higher level of detail can also be seen in fraction planes made for other materials corresponding to roof top coverings, road surfaces, waterways and vegetation areas. The results from examining all of the fraction planes indicate that the sharpened low-spatial-resolution hyperspectral image offers significantly improved capability for scene classification.

The process was repeated for two vegetation endmembers. These two endmembers can be identified as vegetation due to the sharp rise in the radiance at approximately 720 nm. The fraction planes are shown for the application of N-FINDR to both the original 30m-resolution Hyperion data in Figure 8 and the Hyperion data sharpened by CRISP to the four-meter resolution of Ikonos multispectral data in Figure 9. In these images the full 4 km by 4 km processed area is shown along with a detailed view of a particular area. The see the level of information present within the CRISP sharpened data, these two vegetation fraction planes are compared to the Normalized Difference Vegetation Index

(NDVI) image created from the high-spatial-resolution Ikonos data. While the NDVI shows the presence of vegetation at four-meter resolution, the endmember images separate this vegetation into two classes. While this separation is present in the Hyperion data, only in the CRISP sharpened data can one class be identified with trees. This was confirmed through use of a recent Google[14] image.

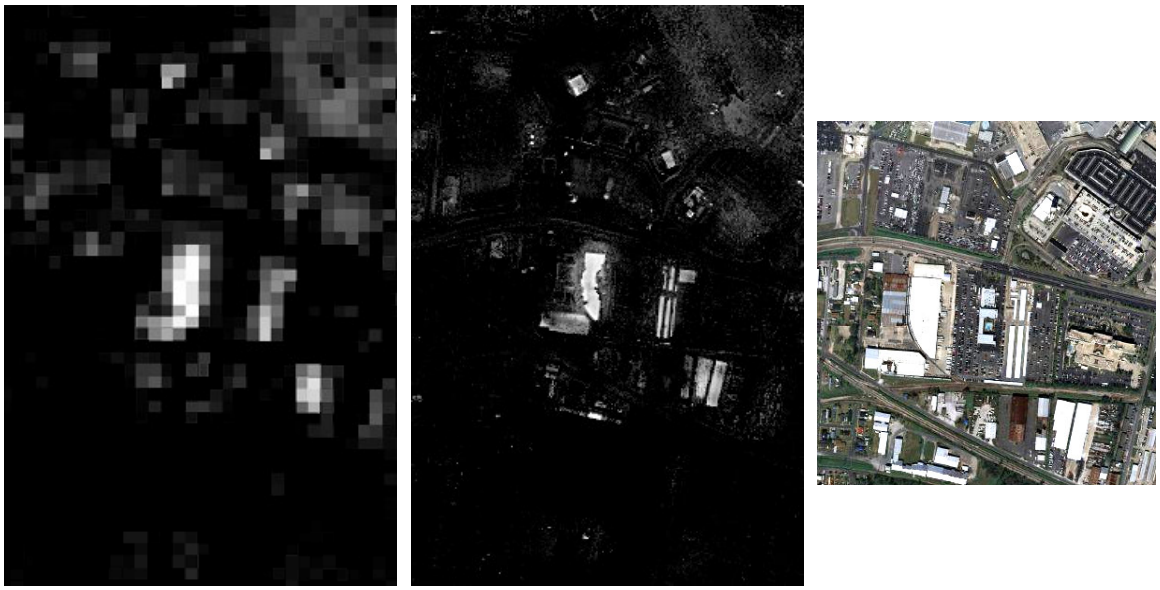

Figure 7. Comparison of the same material fraction plane made from 30m Hyperion data and from CRISP-sharpened data. Note that the material fraction plane shows greater detail than the satellite image.

5. CONCLUSIONS

We demonstrated the CRISP Color Sharpening algorithm on synthetic data for which direct measures of the error in the sharpening process could be made. These studies generally saw the performance to be accurate to within one percent in reflectance. The algorithm was then demonstrated on a variety of multispectral and hyperspectral data combinations. One of these experiments was the spatial resolution enhancement of low-spatial-resolution, high-spectral-resolution Hyperion data acquired in support of the Hurricane Katrina disaster relief with high-spatial resolution multispectral Ikonos data to produce a CRISP-sharpened product that can be used for further hyperspectral analysis in the same manner as high-spatial-resolution hyperspectral data.

ACKNOWLEDGMENTS

This research was sponsored by the Air Force Research Laboratory's Small Business Innovative Research (SBIR) program. The authors acknowledge the support of Michael Schlangen of Technical Research Associates, Inc. and William Weibel of Space Computer Corporation. The data sets used in our study were provided courtesy of the US Geological Survey through the help of Brenda Jones. We also acknowledge the helpful comments of Sherry Olson and colleagues at the MITRE Corporation, and of William Kunze and James Vrabel, both at the National Geospatial-Intelligence Agency.

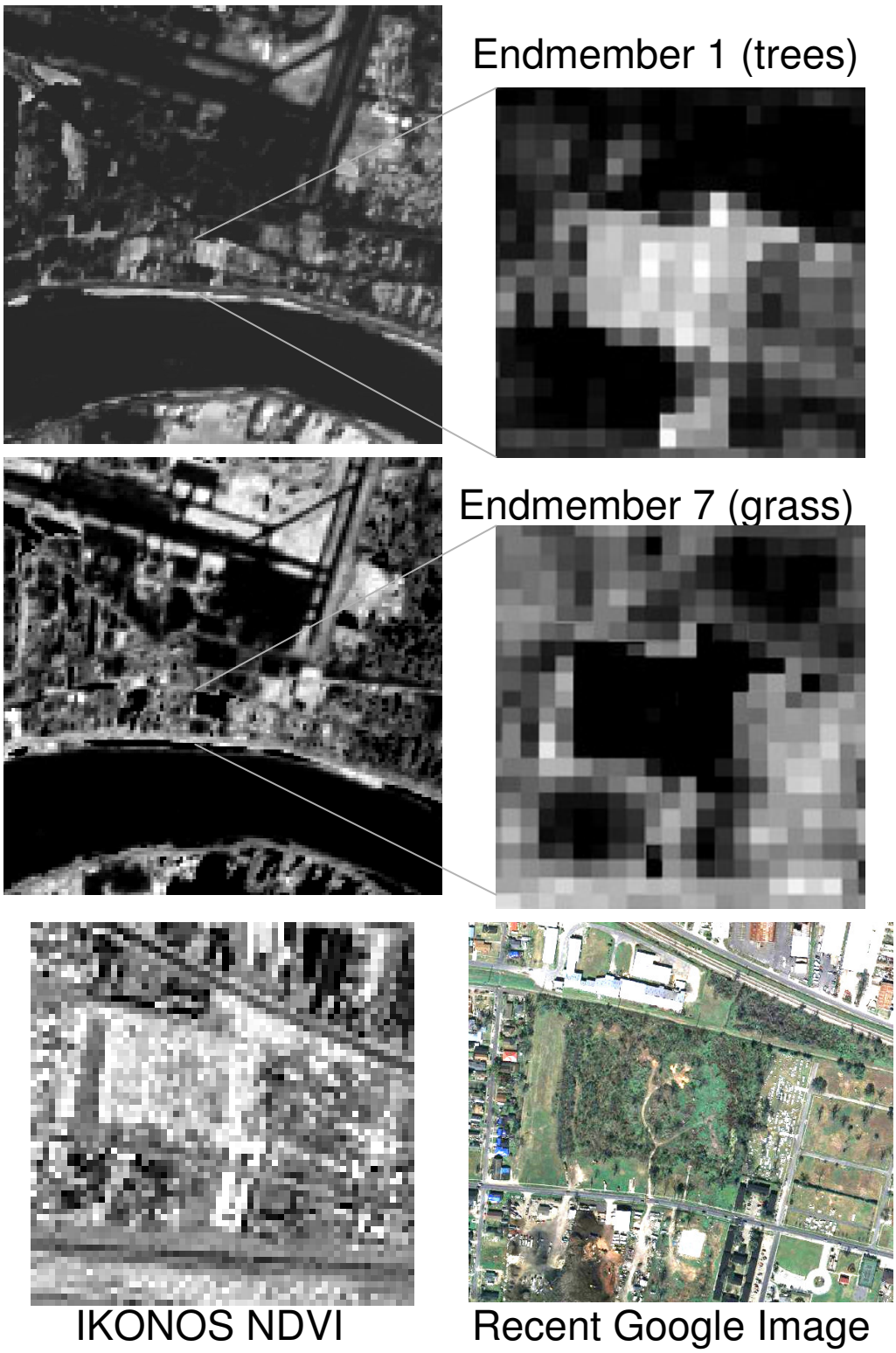

Figure 8. Comparison of the two vegetation endmembers formed from Hyperion 30 m data with an NDVI image from Ikonos and a recent satellite image. Compare to CRISP sharpened Hyperion in Figure 9.

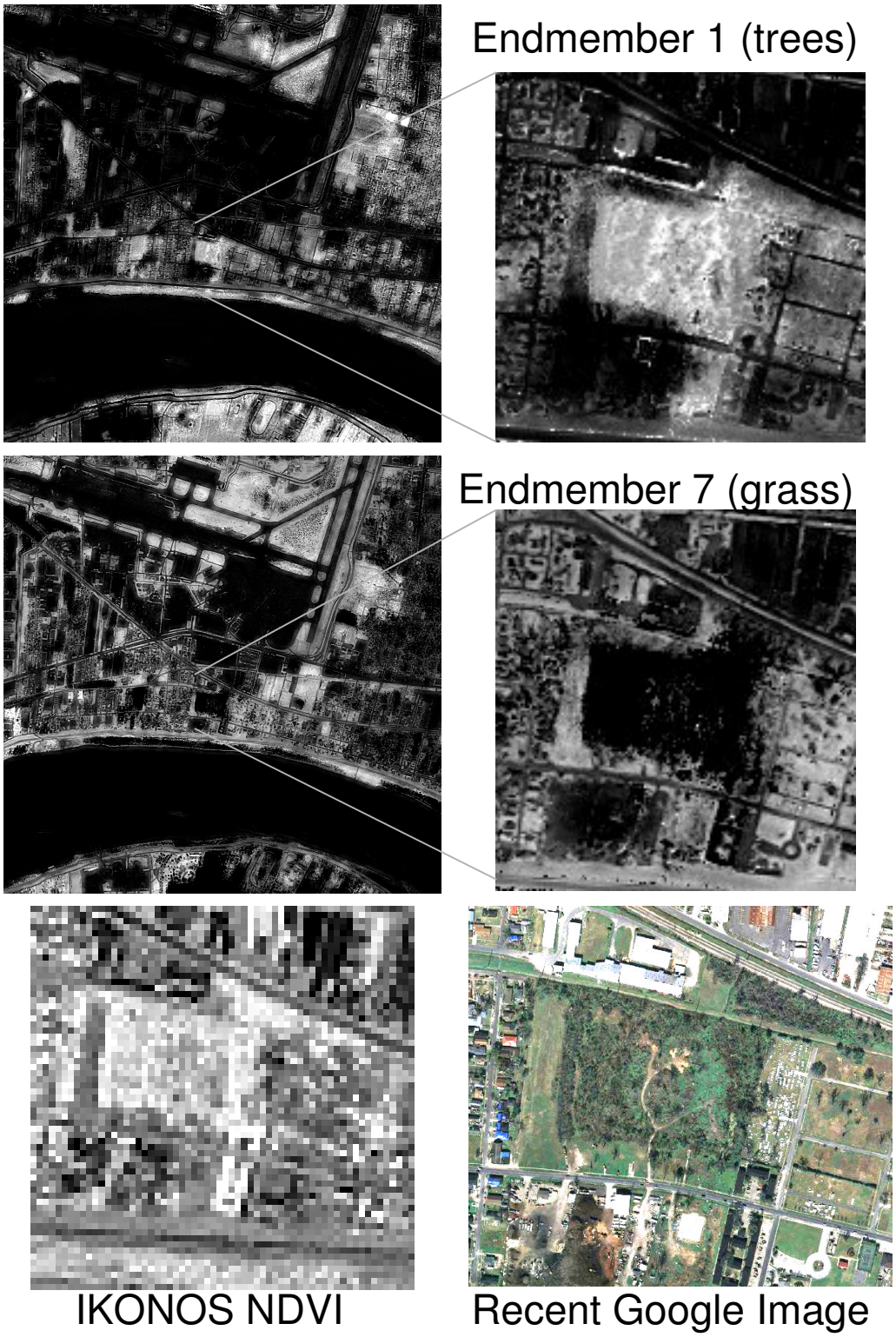

Figure 9. Comparison of the two vegetation endmembers formed from CRISP sharpened Hyperion data with an NDVI image from Ikonos and a recent satellite image.

REFERENCES

[1] Ungar, Stephan G., Jay S. Pearlman, Jeffrey A. Mendenhall and Dennis Reuter, "Overview of the Earth Observing One (EO-1) Mission," IEEE Trans. Geosci. and Remote Sensing, Vol 41, 1149-1159, 2003.

[2] Adams, J.B., M.O. Smith and P.E. Johnson, "Spectral Mixture Modeling: A New Analysis of Rock and Soil Types at the Viking Lander Site," J. Geophysical Research, Vol. 91, pp. 8098-8112, 1986.

[3] Boardman, J.W., K.A. Kruse and R.O. Green, "Mapping target signatures via partial unmixing of AVIRIS data," in: Summaries of the Fifth Annual JPL Airborne Geoscience Workshop, Pasadena, CA, Vol. 1, 1995.

[4] Winter, Michael E., "Fast Autonomous Spectral End-member Determination in Hyperspectral Data," Proceedings of the Thirteenth International Conference on Applied Geologic Remote Sensing, Vol. II, pp 337-344, Vancouver, BC, Canada, 1999.

[5] Richards, J.A. Remote Sensing Digital Image Analysis: An Introduction, Springer-Verlag, Berlin, Germany, 1999.

[6] Green, A., M. Berman, P. Switzer and M D. Craig, "A Transformation for Ordering Multispectral Data in Terms of Image Quality with Implications for Noise Removal," IEEE Transactions on Geoscience and Remote Sensing, Vol. 26, no. 1, pp. 65-74, 1988.

[7] Carper, W. J, T. M. Lillesand and R.W. Kiefer, "The use of intensity hue saturation transformations for merging SPOT panchromatic and multispectral image data," Photogrammetric Engineering and Remote Sensing, 56(4):459-467, 1990.

[8] Vrabel, Jim, 1996, "Multispectral Imagery Band Sharpening Study", Photogrammetric Engineering & Remote Sensing, Vol. 62, No. 9, pp. 1075-1083.

[9] Winter, Michael E., Edwin M. Winter, Scott G. Beaven, and Anthony J. Ratkowski "Hyperspectral Image Sharpening Using Multispectral Data" Proc. of the IEEE Aerospace Conference, Big Sky, MT CD-ROM (2007)

[10] Vane, G., R. O. Green, T. G. Chrien, H. T. Enmark, E.G. Hansen and W. M. Porter, "The Airborne Visible/Infrared Imaging Spectrometer (AVIRIS)," Remote Sensing of the Environment, Vol. 44, pp. 127-143. 1993

[11] Goetz, A. F. H. and V. Srivastava, (1985) "Mineralogical mapping in the Cuprite Mining District, Nevada," Proceedings of the Airborne Imaging Spectrometer Data Analysis Workshop, JPL Publication 85-41, Jet Propulsion Laboratory, Pasadena, CA, p. 22-29.

[12] Abrams, M.J. and R.P. "Ashley, "Alteration mapping using multispectral images - Cuprite Mining District, Esmeralda County, Nevada," U.S. Geological Survey Open File Report 80-367, 1980

[13]. ITT Visualization Systems, ENVI User's Manual

[14]. Winter, Michael, E., "N-FINDR: an algorithm for fast autonomous spectral end-member determination in hyperspectral data," SPIE Conference on Imaging Spectrometry V, SPIE Vol. 3753, pp. 266-275, Denver, Colorado July 1999

[15]. www.google.com